The Korean Journal of Ceramics, **2** [1] 1-10 (1996)

The Applications of Sol-Gel Derived Tin Oxide Thin Films

Sung-Soon Park and John D. Mackenzie

Dept. of Mater. Sci. and Eng., Univ. of California-Los Angeles, Los Angeles, CA 90024, USA
(Received August 11, 1995)

Transparent conducting SnO_2-based thin films have been coated on flat substrates such as fused quartz, and ceramic fiber cloths such as the Nextel and E-glass cloth from tin alkoxides by the sol-gel technique. Also, thin films of alternating layers of SnO_2 and SiO_2 have been fabricated by dip coating. The sheet resistance and average visible transmittance of the films were investigated in the aspect of the applications as transparent electrodes such as liquid crystal displays, photo-detectors and solar cells. The Nextel and E-glass cloths coated with antimony-doped tin oxide (ATO) had sheet resistance of as low as 20 ohm/□ and 120 ohm/□, respectively. The promotion effects of additives as La_2O_3 and Pt on the ethanol gas sensing properties of the films were investigated in the aspects of the applications as an alcohol sensor and a breath alcohol checker. Possible evidence of quantum well effects in the oxide multilayers of SnO_2 and SiO_2 was investigated.

Key words : Sol-gel process, Dip-coating, SnO_2 thin films, Ceramic fiber cloths, Transparent electrodes, Alcohol gas sensor, Quantum well effects, Sheet resistance, Transmittance

I. Introduction

Wide-band-gap semiconductor tin oxide thin films have been attracting much concern since they are highly conducting, transparent, hard, and sensitive to reducing gases. They have many important applications such as liquid crystal displays, photo-detectors, solar cells, gas sensors, and protective coatings.[1-5] Also, they may have potential applications to quantum well optical devices.[6-9] When tin oxide films are used as transparent conducting electrodes for display devices, a low sheet resistance and high transmittance of visible light are required, but for the applications of them as gas sensors, high surface area, that is, ultrafine particles and high porosity are required.

Tin oxide films have been fabricated by a number of techniques, including spray pyrolysis,[10,11] sputtering,[12,13] clemical vapor deposition (CVD)[14,15] and evaporation.[16,17] The main problem encountered in all these techniques has been lack of consistency in the film properties. The properties of the films have been found to depend strongly on the mode of preparation.

It is well known that the sol-gel technique has several advantages, such as excellent homogeneity, easy control of film thickness, ability to coat large and complex-shapes, and simple and low-cost processing, but the most significant advantage of the technique is the ability to produce ultrafine or porous films.[18-21]

In this study we have investgated the dip coating parameters such as solution concentration, the withdrawal speed of substrates from solution, firing temperature, and the number of coating applications and their influences on the thickness and microstructure of the prepared films, which can affect the electrical and optical properties and the gas sensing properties of them. This study shows that the important properties such as sheet resistance, optical transmittance, and gas sensitivity are successfully controlled by controlling the dip coating parameters. The possible evidence of quantum well effects in the alternating layers of SnO_2 and SiO_2 was also investigated.

II. Experimental Details

1. Preparation

Tin oxide thin films were coated on fused quartz substrates by the following process. Tin (IV) ethylhexano-isopropoxide($Sn(OOC_8H_{15})_2(OC_3H_7^i)_2$) was used as a starting material. Pre-cleaned fused quartz substrates were dipped into the mixed solution and were withdrawn with the speeds of 11, 7, and 3 cm/min in air. The films were, then, dried at 100°C for one hour in air. To increase film thickness, dipping process was multifully used. The dried films were fired at 400°C for 10 minutes in air and again dipped into solution. The procedure was repeated to obtain the desired film thickness. Finally, all films were fired at 600°C for one hour in air. Antimony-doped tin oxide (ATO) coatings were deposited on the ceramic cloths by the following process. Tin (IV) isopropoxide ($Sn(OC_3H_7^i)_4$)-isopropanol solution and antimony-butoxide ($Sb(OC_4H_9)_3$) were used as starting materials. Pre-cleaned ceramic cloths were dipped into the solution and impregnated in the solution for 2 min. The coated Nextel cloths and E-glass cloths were fired at 550°C and 500°C, respectively, for 5 minutes in air. The above procedure were repeated to obtain desired thickness of coatings. The coated Nextel

cloths were then fired at 650°C for 5 hours in air. The coated E-glass cloths were fired at 550°C for 15 hours in vacuum.

SnO_2 thin film gas sensors wre prepared by the following process. Tin (IV) ethylhexano-isopropoxide(Sn$(OOC_8H_{15})_2(OC_3H_7^i)_2$) was used as a starting material. Precleaned fused quartz substrates were withdrawn with the speed of 11 cm/min in air. The coated films were dried at 110°C for one hour in air. Finally, for pure SnO_2 and La_2O_3-SnO_2 films, the dried gel films were fired at 600°C for one hour. For Pt-La_2O_3-SnO_2 films, the dried gel films were fired at 600°C for 10 minutes in air. To prevent the formation of platinum oxide, the films were reduced by flowing H_2 gas (30% in Ar) at 300°C for 3 hours. Au electrodes were screen-printed onto the surface of the fired films.

SnO_2/SiO_2 multilayer films have been fabricated by the following process. Tin (IV) ethylhexano-isopropoxide(Sn$(OOC_8H_{15})_2(OC_3H_7^i)_2$) and tetraethylorthosilicate (TEOS, $Si(OC_2H_5)_4$) were used as a precursor for SnO_2 film and SiO_2 film, respectively. After each layer coated alternatively, the sample was fired at 400°C for 15 minutes. To increase the number of layers, the dip coating/heating cycle was repeated. Finally, the sample was fired at 600°C for one hour. Detailed processes for all kinds of samples were discussed in the previous reports.[9,19-21]

2. Measurements

The thickness of the films, which were coated on flat substrates, was measured by a stylus (Dektak IIA, Sloan Co.) and an ellipsometer (AUTOELLER-II, Rudolph Research). Scanning electron microscopy (SEM) was also used to confirm the results and to measure the thickness of the coating on ceramic fibers. SEM was also used to investigate the morphology of the films. Transmission electron microscopy (TEM) was used to investigate the grain size of the films. The refractive index of the films was measured by ellipsometer (λ=6328 Å). Using the measured refractive indices, the porosity of the films was calculated. It is well known that the refractive index of a material is related to its density, which can be lowered by introducing porosity.[22] It is required, however, that the pore size be substantially smaller than the wavelength of the light, and the pore distribution must be homogeneous in order not to affect the light transmission and cause scattering. The porosity and refractive index in this type of material are related by

$$P(\%) = [1-(n_p^2-1)/(n_s^2-1)] \times 100 \quad (1)$$

where p and n_p are the percent porosity and refractive index of porous material, respectively, and n_s is the refractive index of nonporous material.

The chemical composition of the films was analyzed by Auger electron spectroscopy (AES). To obtain semiquantitative analysis of the films, the relative elemental sensitivity approachs was used, which was based on the elemental intensities of the stoichiometric SnO_2 standard sample (compact powder).[23] The Van der Pauw method was used to measure the electrical resistivity and Hall coefficient of the films.[24] On the other hand, the sheet resistance of the ATO coated ceramic cloths was measured by 2 point probe method. Optical transmittance in the wavelength range of 0.2~0.8 μm was measured using a Diode Array Spectrophotometer (HP8452A, Hewlett Packard).

To measure the ethanol gas sensing properties of the films, a pick up resistor was connected in series to the film sensor and adjusted so as to give one-tenth of the resistance of the sensor before expose to ethanol vapor. The dc voltage of 10 V was applied across the circuit and the electrical resistance of the sensor in dry air (R_{air}) and in ethanol vapor (R_{gas}) were measured. The gas sensitivity was defined as the resistance ratio of R_{air}/R_{gas}.

III. Results and Discussion

1. Transparent conducting electrode

1.1 Physical properties

X-ray diffraction pattern indicated that the prepared films started to crystallize at 300°C. The dip coating parameters that influence film thickness are the solution concentration, the withdrawal speed of substrates from the solution, and the firing temperature.[25,26] The control of film thickness is possible only the parameters are suf-

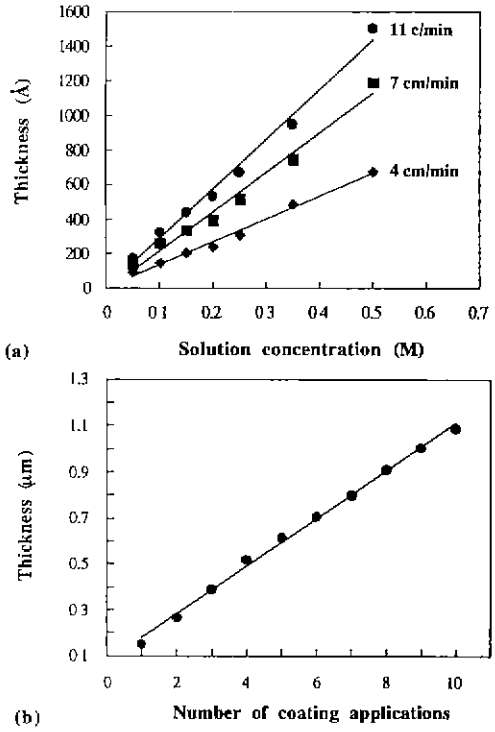

Fig. 1. Dependence of SnO_2 film thickness on (a) solution concentration and (b) the number of coating applications.

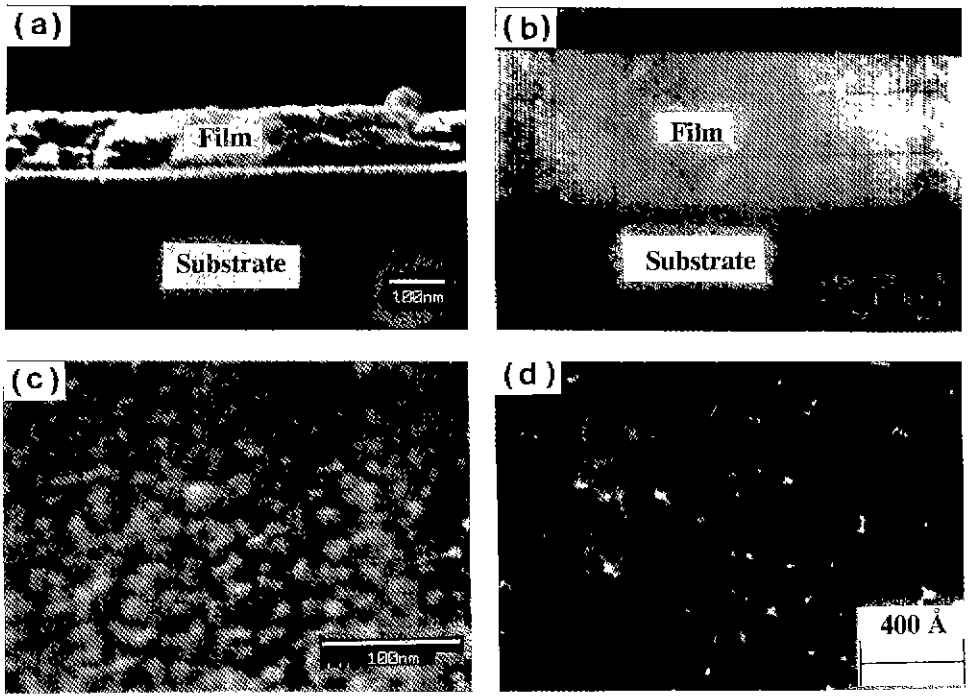

Fig. 2. SEM micrographs of SnO_2 films of (a) lateral fracture surface of singledipped films, (b) lateral fracture surface of multidipped films, (c) surface of singledipped films, and (d) TEM micrograph of (c).

ficiently known. An example is the relationship between thickness, t, and the withdrawal speed, u. In the present work, we obtained the relationship of $t \alpha u^{2/3}$. Since the polycondensation reaction rate of hydrolyzed tin alkoxide is enhanced with increasing solution concentration, it was expected that the resultant layer would be thicker films by using solutions with higher concentration. It was found that there was a linear relationship between the film thickness and the solution concentration (Fig. 1(a)). Since the solution concentraiton of 0.5 mole produces good microstructure, electrical proprties, and optical transimittance, the dependence of film thickness on firing temperature and the number of coating applications was investigated for the films dipped into the solution of 0.5 mole with the withdrawal speed of 11 cm/min. Film thickness decreased with increasing firing temperature. It was also found that there was a linear relationship between the film thickness and the number of coating applications (Fig. 1(b)). Film thickness increased with an interval of about 0.105 μm from 0.15 to 1.09 μm by increasing the number of coating applications from 1 to 10. However, in the present work, the thickness in the range 100~1500 Å, and 0.15~1.09 μm could be successfully controlled by singledipping and multidipping process, respectively. Fig. 2 shows SEM micrographs of singledipped and multidipped SnO_2 films and TEM micrograph of the singledipped films. As shown in the figure, the singledipped and multidipped films have very uniform thickness. The thickness measured by SEM showed good agreement with the thickness values measured by stylus and ellipsometer. The grain size of

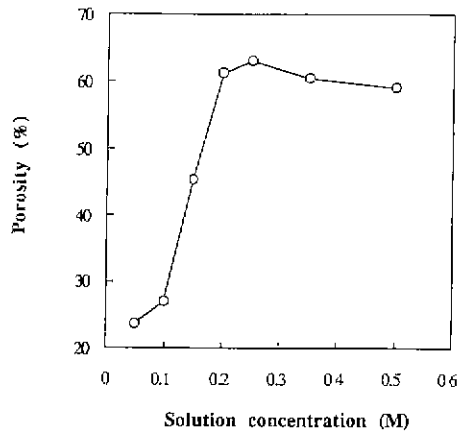

Fig. 3. Dependence of film porosity on solution concentration for singledipped SnO_2 films.

the singledipped films coated with the concentration of 0.5 mole was uniform and about 100 Å.

The dependence of porosity on the solution concentration was investigated for the singledipped films (Fig. 3). As confirmed in SEM micrographs of the prepared films (Fig. 2), the pore size was much smaller than the wavelength of the light, 6328 Å, and the pore distribution was homogeneous. Thus, to calculate the porosity of the films, we used Eq. (1). The refractive index value of singlecrystal SnO_2 (n_s=2.041 at λ=6328 Å) was used for the required refractive index value of nonporous material. The film porosity increased from 24 to 64% with increasing the concentration from 0.05 to 0.25

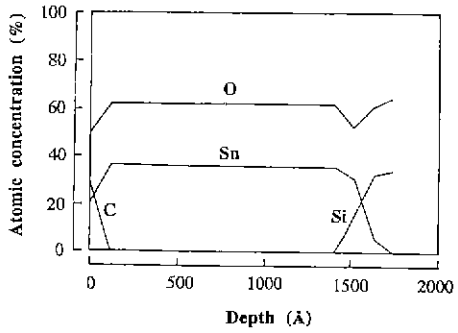

Fig. 4. Typical auger depth-profile of singledipped SnO_2 films.

mole but gradually decreased above 0.25 mole. As confirmed in thermal gravimetric analyzer (TGA), these high film porosity were due to the evaporation of ethylhexanoic acid produced by hydrolysis reaction and the decomposition of partially hydrolyzed residual alkoxy groups in the high temperature range 350~450°C. As discussed in previous report[27], this microstructure evolution of the singledipped films with the solution concentration seems to be due to the competition between the solvent evaporation and the agglomeration of monosized gels. However, the porosity of the multidipped films decreased with increasing the number of coating applications. It was believed that the open pores of the first layer were filled with tin alkoxide solution when the second layer was applied. This filling of open pores and the repeated firing of the films at 400°C seemed to result in the densification of the films and to decrease film porosity with increasing the number of coating applications.

1.2 Electrical and optical properties

Fig. 4 shows a representative Auger depth-profile of the singledipped films. As shown in the figure, the film had uniform composition profile through the film depth, and only carbon existed on the surface of the films as impurities. However, the x value in the prepared SnO_{2-x} films was in the range of 0.02~0.09. This result confirmed that the conductivity of SnO_2 was primarily due to its nonstoichiometry, that is, oxygen deficiency. The oxygen deficiency is caused by oxygen vacancies or interstitial tin atoms.[28] Hall measurement showed that the films were n-type semiconductor. Fig. 5 shows the dependence of resistivity σ, carrier concentration n, and mobility μ of free carriers (measured at room temperature) on the solution concentration for the singledipped films and on the number of coating applications for the multidipped films. The resistivity of the singledipped films dropped from 3 to 7×10^{-1} ohm-cm by increasing the solution concentration up to 0.35 mole and it leveled off as the concentration increased. Also the charge carrier concentration sharply increased from 10^{18} to 8×10^{19} cm^{-3} by increasing the solution concentration up to 0.35 M and it again leveled off as the solution concentration increased, but the mobility was almost constant. Thus, the tendency of the resistivity change with the solution concentration was due to the dependence of the carrier concentration on the solution concentration. As confirmed by SEM micrographs, the particle size of the films increased with increasing solution concentration. Thus, the change of carrier concentration seemed to be due to the increased particle size with the solution concentration, although the change of particle size did not affect the mobility seriously. The mobility ranging from 0.9 to 1.1 cm^2/v-sec was small as compared to the corresponding value of 5~30 cm^2/v-sec for the tin oxide films with a mean particle size of 200~300 Å and seemed to be due to grain boundary scattering.[29]

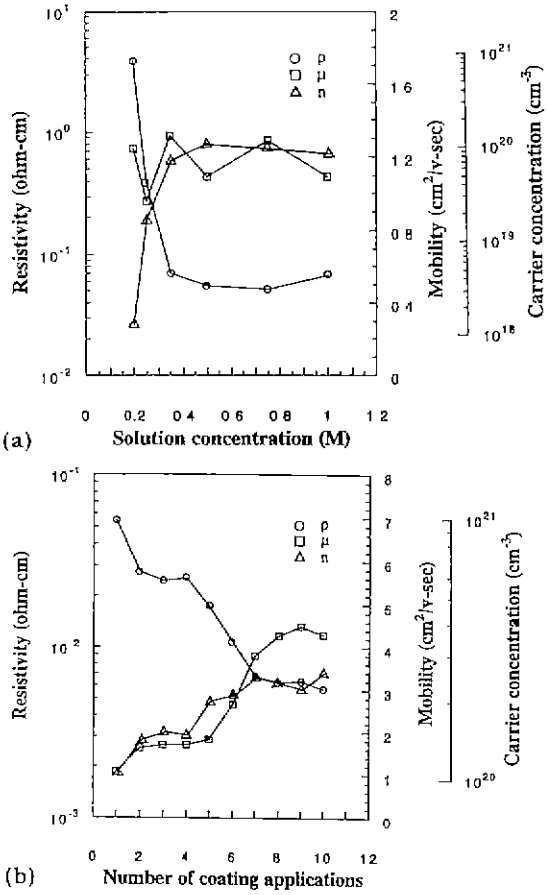

Fig. 5. Dependence of resistivity ρ, carrier concentration n, and mobility μ of free carriers on (a) solution concentration for singledipped films and (b) the number of coating applications for multidipped films.

The resistivity of the multidipped films dropped from 5.5×10^{-2} to 5.7×10^{-3} ohm-cm by increasing the number of coating applications from 1 to 10. On the other hand, both the carrier concentration and mobility increased with increasing the number of coating applications. As discussed earlier the open pores of the first layer would be filled with tin alkoxide solution when the second layer was applied. This filling of open pores and the repeated firing of the films at 400°C seemed to result in the densification of the films and to increase the carrier concentration and mobility with increasing the number of coating applications.

Fig. 6 shows the dependence of the sheet resistance and average visible transmittance for the multidipped films

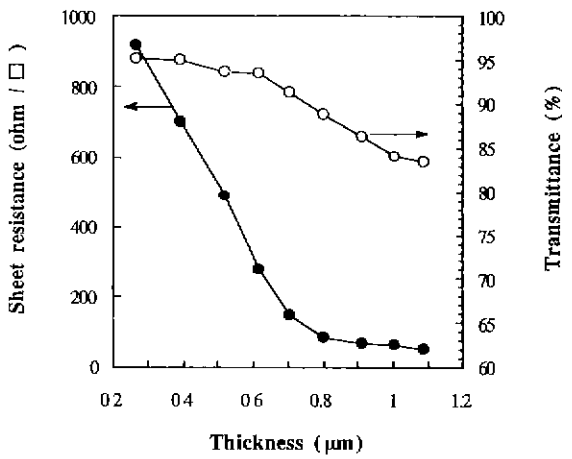

Fig. 6. Dependence of sheet resistance and visible transmittance on thickness for multidipped SnO_2 films.

Table 1. The Solubility of Metal Alkoxides

Metal alkoxides		Solvent	Solubility (g/100 ml)
Antimony butoxide	$Sb(OC_4H_9)_3$	isopropanol	completely soluble
Tin (IV) isopropoxide	$Sn(OC_3H_7^i)_4$	isopropanol	> 10
Zinc tert-butoxide	$Zn(OC_4H_9)_2$	ether	< 10
Cadmium tert-butoxide	$Cd(OC_4H_9)_2$	hexane	< 5
Indium isopropoxide	$In(OC_3H_7^i)_3$	isopropanol	< 1

on film thickness. Both the sheet resistance and the transmittance decreased significantly with increasing the thickness. However, we could obtain sheet resistance as low as 52~85 ohm/□ (or a resistivity of about 6×10^{-3} ohm-cm) and average visible transmittance of 84~89%.

2. Protective and conducting coatings on ceramic fiber cloths

It has been reported that the resistivity of transparent and conducting oxide films, such as indium-doped tin oxide (ITO), zinc oxide (ZO) and cadmium-doped in oxide (CTO), ranged from 10^{-4} to 10^{-2} ohm-cm.[1,2,29,30] Depending on the fabrication technique, the resistivity of the same system can have the difference of 2~3 orders.

Preparation of ceramics via the sol-gel process has several requirements. One of the important requirements is the solubility of metal alkoxides in normal organic solvents. Table 1 shows the solubility of various metal alkoxides and indicates that tin alkoxides have the highest solubility. Antimony-doped tin (IV) oxide (ATO) will be one we should work on.

Fig. 7 shows the typical SEM micrographs of the cross section and the surface for the ATO coated Nextel cloths, which were fired at 750°C for 6 hours in air. The coatings were not so smooth. In this coating process, the important parameters that could control the physical properties of the coatings were antimony concentration, the number of coating applications, impregnation time, firing temperature, firing time, and firing atmospheres. As-

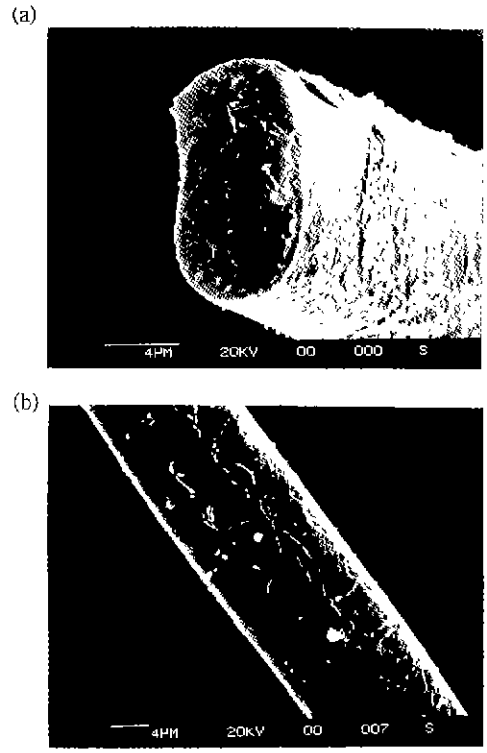

Fig. 7. SEM micrographs of (a) the cross section and (b) the surface for the ATO coated Nextel cloths.

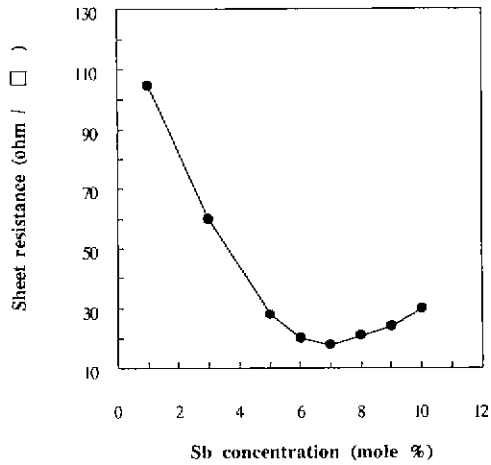

Fig. 8. Dependence of sheet resistance of the ATO coated Nextel cloths on Sn concentration.

suming that all tin isopropoxide ($Sn(OC_3H_7^i)_4$) and antimony-butoxide ($Sb(OC_4H_9)_3$) would be hydrolyzed to form tin oxide (SnO_2) and antimony oxide (Sb_2O_3), respectively, antimony concentration was decided. Fig. 8 shows the dependence of the sheet resistance of the ATO coated Nextel cloths on antimony concentration, which were coated 5 times and fired at 650°C for 5 hours in air. The sheet resistance of the Nextel cloths decreased with increasing antimony concentration; at 7 mole %, the cloths had the lowest sheet resistance of 18 ohm/□; then the sheet resistance slightly increased with increasing antimony concentration. It was illustrated that the doping

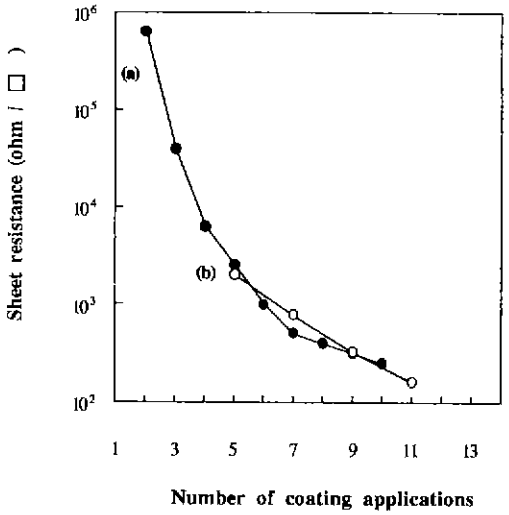

Fig. 9. Dependence of sheet resistance of the ATO coated ceramic cloths on the number of coating applications: (a) the Nextel cloths; (b) the E-glass cloths.

of antimony into SnO_2 could enhance the conductivity due to the increase in the carrier concentration.[29] In our experiment, the sheet resistance of the ATO coated cloths decreased sharply with increasing antimony concentration but increased at still higher concentration (> 7 mole % Sb). The sharp decrease of the sheet resistance at low antimony concentration seemed to be due to the increase in the carrier concentration. The increase in the sheet resistance at higher antimony concentration is suggested to be attributed to impurity scattering, precipitation of Sb_2O_5 or an increased disorder. The actual mechanism is under investigation.

The dependence of the sheet resistance of the ATO coated Nextel and E-glass cloths on the number of coating applications was measured (Fig. 9). The ATO coated Nextel cloths were fired at 650°C for 5 hours in air. In the case of the ATO coated E-glass cloths, they were fired at 550°C for 15 hours in vacuum to prevent the ionosorption of oxygen on the surface of the ATO coating, which decrease the concentration of conduction electrons in the coating. The sheet resistance of the coated cloths had an initial rapid drop that tapered off increasing number of coating. It has been known that a higher firing temperature and longer firing time would produce increasingly crystalline coatings that should have higher conductivity. It was found that the sheet resistance of the cloths decreased with increasing firing temperature and longer firing time led to lower the sheet resistance of the coated Nextel cloths. Based on the above experimental results, the optimum conditions to achieve the highest conductivity of ATO coatings have been determined. However, the Nextel and E-glass cloths of 12″ × 12″ were successfully coated. The sheet resistance of the Nextel and E-glass cloths were 20 ohm/□ and 120 ohm/□, respectively.

3. *Gas sensors*

3.1 *Effects of thickness and microstructure*

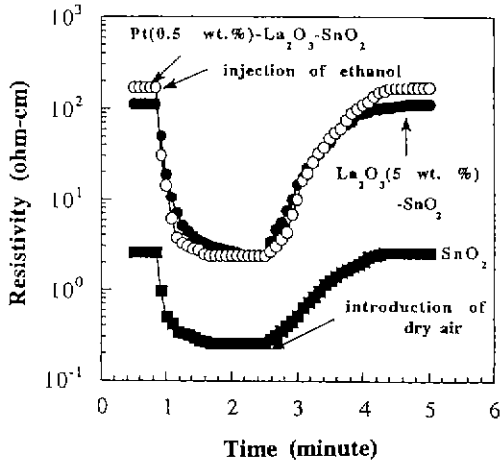

Fig. 10. Response transients on switching on and off 1000 ppm C_2H_5OH in dry air at 300°C for pure SnO_2, La_2O_3 (5 wt.%)-SnO_2, and Pt(0.5 wt.%)-La_2O_3(5 wt.%)-SnO_2 film.

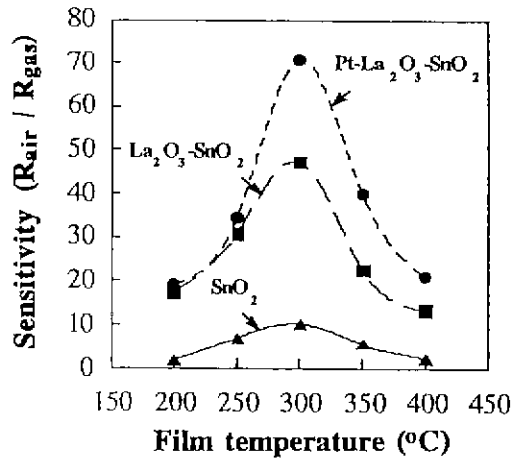

Fig. 11. Temperature dependence of sensitivity to 1000 ppm C_2H_5OH in dry air at 300°C for pure SnO_2, La_2O_3 (5 wt.%)-SnO_2, and Pt(0.5 wt.%)-La_2O_3(5 wt.%)-SnO_2 film.

Fig. 10 shows the response transients on switching on and of 1000 ppm C_2H_5OH in dry air at 300°C for the films with the thickness of about 700 Å. As shown in the figure, the response transients of the La_2O_3 (5 wt.%)-SnO_2 and Pt (0.5 wt.%)-La_2O_3 (5 wt.%)-SnO_2 films are similar to the one of the pure SnO_2 film. Upon switching on C_2H_5OH, the films reached saturated values in about one minute, and upon switching off, they returned to original values in about 2 minutes. The resistivity of the single and doubly loaded film in dry air was 1.2×10^2 ohm-cm and 1.8×10^2 ohm-cm, respectively. The values are larger than the one of pure SnO_2 film, 2.7×10^0 ohm-cm.

Fig. 11 shows the temperature dependence of sensitivities of the above three films on switching on 1000 ppm C_2H_5OH. Like the pure SnO_2 film, the singly and doubly loaded film exhibited the maximum sensitivity at 300°C. This indicated the equilibrium density of the ionosorbed oxygen O^-_{ads} or O^{2-}_{ads} would be maximum at 300°C. On the other hand, the response time decreased with increasing operating temperature. This seems to be

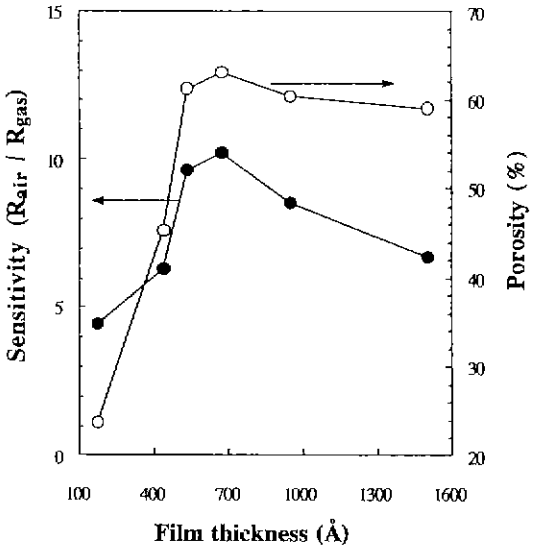

Fig. 12. Dependence of sensitivity to 1000 ppm C_2H_5OH in dry air at 300°C and porosity on thickness for pure SnO_2 films.

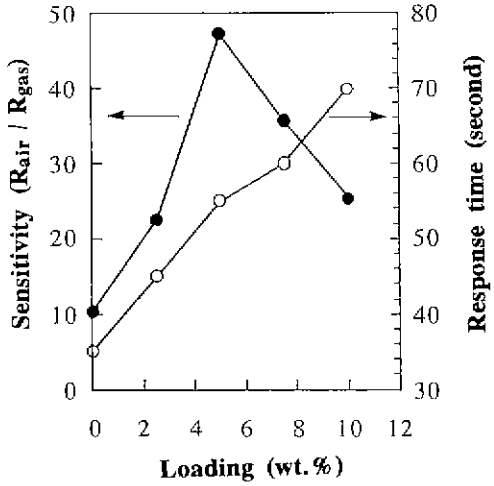

Fig. 13. Dependence of sensitivity and 90% response time on the amount of La_2O_3 to 1000 ppm C_2H_5OH in dry air at 300°C for La_2O_3-SnO_2 films.

due to the accelerated oxidation reaction of C_2H_5OH with increasing temperature.

The effects of additives on the ethanol gas sensing properties of the films will be discussed later. Fig. 12 shows the dependence of ethanol gas sensitivity to 1000 ppm C_2H_5OH at 300°C and porosity on film thickness for pure SnO_2 films. The curve in the figure shows that maximum sensitivity appears at the film thickness of 700 Å and below the thickness, the sudden decrease of the sensitivity with decreasing thickness follows the sudden decrease of the porosity with decreasing thickness. There are scant data in the literature for the thickness dependence of ethanol gas sensitivity. H_2 gas sensitivity dependence of SnO_2 films on the thickness was measured by Cha et al.[31] They found maximum sensitivity at a film thickness of 730 Å for undoped SnO_2 films and in the thickness range 325~375 Å for Pd-SnO_2 films. Windischman et al.[32] suggested a single-crystal thin film model, which excludes the effects of microstructure. According to their model, the SnO_2 film sensor functions best when film thickness becomes equal to the thickness of the depletion layer generated by the ionosorbed oxygen. However, their model do not explain the sudden sensitivity drop below the critical film thickness. On the other hand, Cha et al.[31] suggested that the sudden sensitivity drop seemed to be due to the fact that a film having a thickness below a certain value became less sensitive by loosing crystallinity. Their suggestion is thought to be really applicable for singlecrystal films or the polycrystal films with same microstructure, but not enough for the polycrystal films with different microstructure, which can affect gas sensing properties. The grain size of the prepared films did not increased seriously with increasing film thickness, but film porosity decreased sharply with decreasing the thickness. Thus it seemed that, in this case, the microstructure effects would be mainly due to not the grain size change but the porosity change with film thickness. However, below the thickness of 700 Å, the sharp decrease of the porosity would result in the decreased surface area, that is, the decreased number of the available sites for the oxidation reaction of ethanol molecules and again would lead to the decreased sensitivity with decreasing the thickness. Detailed explanation about the thickness effects was given in previous report.[27]

3.2 Effects of additives

A series of films with various La_2O_3 concentratin in SnO_2 was investigated (Fig. 13). As shown in the figure, the sensitivity was markedly enhanced by loading with La_2O_3, and the highest sensitivity at 300°C was obtained by loading with 5 wt.%. For the La_2O_3 (5 wt.%)-SnO_2 film, the sensitivity to 1000 ppm C_2H_5OH increased from 10.2 to 47.3. As discussed in previous report[33], this promotion effect of La_2O_3 is due to the preferential dehydrogenation of C_2H_5OH on the basic surface of SnO_2 particles and the increased surface area of SnO_2 particles. The sensitivity further increased by loading with 0.5 wt.% Pt from 47.3 to 70.7. This promotion effect seemed to be due to that the noble metal, Pt could activate the spill-over of C_2H_5OH to facilitate its catalytic oxidation on SnO_2 particles.

Unlike the sensitivity, the response time of La_2O_3 (5 wt.%)-SnO_2 films was larger than that of pure SnO_2 film, but the response time could be decreased by loading with Pt. For the La_2O_3 (5 wt.%)-SnO_2 film, the 90% response time was 55 seconds at 300°C, while for the Pt-La_2O_3 (5 wt.%)-SnO_2 film, it was 35 seconds at 300°C, the same as the 90% response time for pure SnO_2. It appears that the increased response time caused by loading with La_2O_3 is completely removed by loading with Pt.

In the aspect of commercial applications, the most important property for the gas sensor is the dependence of the sensitivity on gas concentration. Large and linear dependence is required for reasonable sensing. Theoretically the ethanol gas sensitivity is defined as a power

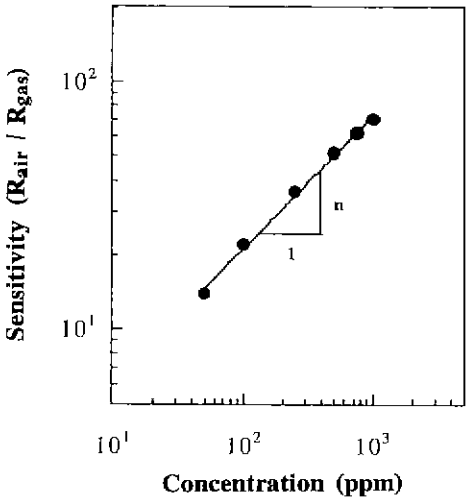

Fig. 14. Dependence of sensitivity on C_2H_5OH concentration at 300°C for Pt (0.5 wt.%)-La_2O_3 (5 wt.%)-SnO_2 film

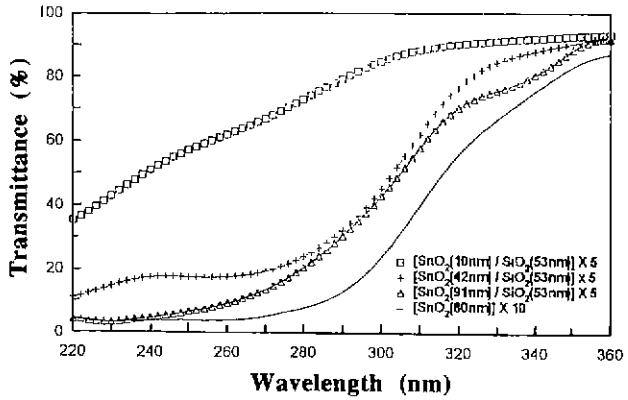

Fig. 15. UV-visible transmittance spectra of the films. Top three curves related to SnO_2/SiO_2 multilayer films with different SnO_2 thickness and the spectrum of a sample of pure SnO_2 films plotted at the bottom for comparision.

law, $S=[C_2H_5OH]^n$, where n is 0.5.[17] Fig. 14 shows the dependence of sensitivity of Pt (0.5 wt.%)-La_2O_3 (5 wt %)-SnO_2 film on ethanol concentration at 300°C. Using a standard linear regression method, the exponent value, 0.56 was calculated. The experimental value showed a good agreement with the theoretical value. Thin film gas sensors can detect gas much quickly and can be integrated as microsensors. A breath alcohol checker is said to be designed to give warning for a drunken driver when the ethanol concentration of his breath exceeds 70 ppm. The sensitivity of the present film sensor at 70 ppm C_2H_5OH was as high as 18 being sensitive enough to be a breath alcohol checker.

4. Possibility of quantum well effect

It is well known that epitaxial AlGaAs/GaAs multilayer films are good candidates for uses in quantum well optical devices.[34,35] Thus far, such devices have been developed only for covalent semiconductors. The possibility of the quantum well effects of SnO_2/SiO_2 oxide multilayer films was investigated. Optical transmittance

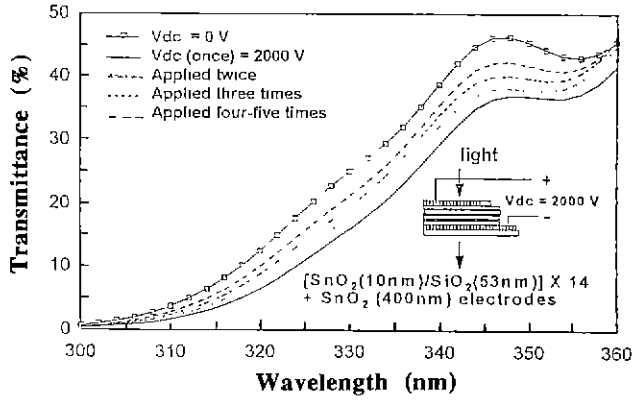

Fig. 16. UV-visible transmittance spectra of the SnO_2/SiO_2 multilayer films with and without an electric field.

of the multilayer films was measured to gain insight into their optical properties. Fig. 15 shows the UV-visible transmission spectra of the SnO_2/SiO_2 multilayer films. A decrease in the thickness of SnO_2 layers, from 901 to 100 Å, led to a shift of the absorption edge to shorter wavelenths. Additional work on the phase and structural changes in the films is needed, in order to check if the phenomenon is related to quantum well effects.

To study the effect of electrical field on the films, multilayer structures of 14 pairs of SnO_2 (100 Å) and SiO_2 (530 Å) layers were sandwiched with SnO_2 electrodes (4000 Å). A voltage of 2000 V was applied across the multilayer layers through the electrodes. The electrical field changed the transmission (Fig. 16). Applying the electrical field again, the transmission curve shifted back closer in its original position. Work is currently under way in order to investigate the causes of this effect and whether it is related to a quantum well mechanism such as the Quantum Confined Stark Effect.

IV. Conclusion

Transparent conducting SnO_2-based thin films have been coated on fused quartz substrates and ceramic fiber cloths such as the Nextel and E-glass cloth of $12'' \times 12''$ by the sol-gel technique. Also, thin films of alternating layers of SnO_2 and SiO_2 have been fabricated by dip coating. The prepared films of sheet resistance as low as 52~85 ohm/□ and average visible transmittance of 84~89% seems to one of the best candidates for the application of transparent conducting electrodes. The sheet resistance of the antimony-doped tin oxide (ATO) coated Nextel and E-glass cloths was as low as 20 ohm/□ and 120 ohm/□, respectively. The sensitivity of pure SnO_2 film further increased by loading with Pt and La_2O_3. The sensitivity of the Pt (0.5 wt.%)-La_2O_3 (5 wt.%)-SnO_2 film sensor at 70 ppm C_2H_5OH was as high as 18, being sensitive enough to be a breath alcohol checker. With decreasing the thickness of SnO_2 layer and applying electrical field, the transmission spectra of the multilayer of SnO_2 and SiO_2 were changed. Whether the causes of these effects are related to quantum well effects or not is not clear. Further

work is currently under way to investigate if their nature is related to quantum well effects.

Acknowledgement

The authors are grateful to the Northrop corporation and the Air Force office of Scientific Research, Directorate of Chemical and Materials Science for supporting these researches.

References

1. K. L. Chopra, S. Major and D. K. Pandya, "Transparent Conductors-a Status Review," *Thin Solid Films*: Review Paper, **102**, 1 (1983).
2. A. L Dawar and J. C. Joshi, "Semiconducting Transparent Thin Films: Their Properties and Applications," *J Mat. Sci*: Review, **19**, 1 (1984).
3. J. C. Manifacier, L. Szepessy, J. F. Bresse and M. Perotin, "In_2O_3: (Sn) and SnO_2: (F) Films-Applications to Solar Energy Conversion, Part II-Electrical and Optical Properties," *Mat. Res. Bull.*, **14**, 163 (1979).
4. T. Seiyama, Chemical Sensor Technology: pp. 39-53, Elsevier, New York, 1988.
5. K. Ihokura and J. Watson, the Stannic Oxide Gas Sensor, pp. 129-168, CRC Press, Ann Arbor, 1994.
6. L. Esaki, "A Bird's-Eye View on the Evolution of Semiconductor Superlattices and Quantum Wells," *J. Quantum Electronics*, **QE-22**[9], 1611 (1986).
7. D. A. B. Miller, D. S. Chemla and T. C. Damen, "Novel Hybrid Optically Bistable Switch: The Quantum Well Self-Electro-Optic Effect Device," *Appl. Phys. Lett.*, **45**[1], 13 (1984).
8. T. H. Wood, "Multiple Quantum Well Devices for Monolithic Integrated Optoelectronic," SPIE Proc., Quantum Wells and Superlattices in Optoelectronic Devices and Integrated Optics., 861, 1 (1987).
9. Q. Wu, Y. Xu, S. S. Park, E. P. Bescher and J. D. Mackenzie, "Optical Properties of Multilayer Thin Films," *Ceram. Trans. (Sol-Gel Sci. and Tech.)*, **55**, 235 (1995).
10. J. C. Manifacier, L. Szepessy, J. F. Bresse and M. Perotin, "In_2O_3.(Sn) and SnO_2: (F) Films-Applications to Solar Energy Conversion, Part I-Preparation and Characterization," *Mat. Res. Bull.*, **14**, 163 (1979).
11. H. D. Waal and F. Simonis, "Tin Oxide Coatings: Physical Properties and Applications," *Thin Solid Films*, **77**, 253 (1981).
12. J. F. Smith, A. J Aronson, D. Chen and W. H. Class, "Reactive Magnatron Deposition of Transparent Conductive Films," *Thin Solid Films*, **72**, 469 (1980).
13. T. Karasawa and Y. Miyata, "Electrical and Optical Properties of Indium Tin Oxide Thin Films Deposited on Unheated Substrates by D. C. Reactive Sputtering," *Thin Solid Films*, **223**, 135 (1993).
14. J. C. Lou, M. S. Lin, J J. Chyi and J. H. Shieh, "Process Study of Chemically Vapor-Deposited SnO_x (x=2) Films," *Thin Solid Films*, **128**, 181 (1985).
15. R. D. Tarey and T. A. Raju, "a Method for the Deposition of Transparent Conducting Thin Films of Tin Oxide," *Thin Solid Films*, **128**, 181 (1985).
16. D. W. Lane, J. A. Coath, K. D. Rogers, B. J. Hunnikin and H. S. Beldon, "Optical Properties and Structure of Thermally Evaporated Tin Oxide Films," *Thin Solid Films*, **221**, 262 (1992).
17. H. Ogawa, M. Nishikawa and A. Abe, "Hall Measurement Studies and an Electrical Conduction Model of Tin Oxide Ultrafine Particle Films," *J. Appl. Phys.* **53**, 4448 (1982).
18. L. C. Klein, Sol-Gel Technology for Thin Films, Fibers, Preforms, Electronics, and Specially Shapes; pp. 49-91, Noyes publications, New York. 1988.
19. S S. Park, H. Zheng and J. D. Mackenzie, "Sol-Gel Derived Antimony-Doped Tin Oxide Coatings on Ceramic Cloths," *Mater. Lett.*, **22**, 175 (1995)
20. S. S. Park and J. D. Mackenzie, "Sol-Gel-Derived Tin Oxide Thin Films," *Thin Solid Films*, **258**, 268 (1995).
21. S. S. Park and J. D. Mackenzie, "Microstructure Effects in Multidipped Tin Oxide Films," *J. Am. Ceram. Soc.*, **78**, 2669 (1995).
22. B. E. Yoldas, "Investigation of Porous Oxides as an Antirefractive Coating for Glass Surface," *Appl Opt.* **19**, 1425 (1980).
23. S. Hofman, "Characterization of Nitride Coatings by Auger Electron Spectroscopy and X-ray Photoelectron Spectroscopy," *J. Vac. Sci. Technol.*, **A4**, 2789 (1986).
24. L. J. Van Der Pauw, "A Method Specific Resistivity and Hall Effects of Discs of Arbitrary Shape," *Philips Res. Rep.*, **13**, 1 (1958).
25. C. J. Brinker, G. C. Frye and C. S. Ashley, "Fundamentals of Sol-Gel Dip Coating," *Thin Solid Films*, **201**, 97 (1991).
26. C. J. Brinker, A. J. Hurd, P. R. Schunk, G. C. Frye and C. S. Ashley, "Review of Sol-Gel Thin Film Formation," *J. of Non-Cryst. Solids*, **147 & 148**, 424 (1992).
27. S. S. Park and J. D. Mackenzie. "Thickness and Microstructure Effects on Alcohol Sensing of Tin Oxide Thin Films," accepted to be published in *Thin Solid Films*, 1995.
28. Z. M. Jarzebski and J. P. Marton, "Physical Properties of SnO_2 Materials I. Preparation and Defect Structure," *J. Electrochem. Soc.*: Reviews and News, **123**, 199c (1976).
29. E. Shanti, V. Dutta, A. Banerjee and K. L. Chopra, "Electrical and Optical Properties of Undoped and Antimony-Doped Tin Oxide Films," *J. Appl. Phys.*, **51**, 6243 (1980).
30. C. A. Vincent, "the Nature of Semiconductivity in Polycrystalline Tin Oxide," *J. Electrochem. Soc.* **119**, 515 (1972).
31. K. H Cha, H. C. Park and K. H. Kim, "Effects of Palladium Doping and Film Thickness on the H_2-gas Sensing Characteristics of SnO_2," *Sensors and Actuators*, **B21**, 91 (1994).
32. H. Windischman and P. Mark, "A Model for the Operation of a Thin Film SnO_x Conductance-modulation Carbon Monoxide Sensor," *J Electrochem. Soc.*, **126**, 627 (1979).
33. S. S. Park, H. Zheng and J. D. Mackenzie, "Ethanol Gas Sensing Properties of SnO_2-Based Thin-Film Sensors Prepared by the Sol-Gel Process." *Mater. Lett.*, **17**, 346 (1993).

34. L. Esaki, "A bird's-eye View on the Evolution of Semiconductor Superlattices and Quantum Wells," *IEEE J. Quantum Electronics,* **QE-22**, 1611 (1986)
35. D. A. B. Miller, D. S. Chema and T. C. Damen, "Novel Hybrid Optically Bistable Switch: The Quantum well Self-electro-optic Effect Device," *Appl. Phys. Lett.*, **45**, 13 (1984)